Toronto Metropolitan University

AER722 Aeroelasticity

An Analytical Study of a 2D Airfoil as an Aeroelastic Model

Final Report

Authors: Aman Gilani, Muhammad Mohsin Mukhtar

Abstract

In this project, a two-dimensional, two degree-of-freedom aeroelastic model in a wind tunnel subjected to uniform flow was analyzed. The aeroelastic system consisted of 2 translational springs, 1 helical spring, 1 mechanical damper, and a mass element. Utilizing Newton's Equations and Lagrange Mechanics, the equation of motion of the aeroelastic system was obtained. It was found that both approaches gave the same results for the equation of motion. Using the equation of motion and Routh stability criteria, the stability of the system was determined at various speeds. In addition, the critical flutter speed was calculated. On MATLAB, the stiffness and location of the springs was varied to determine their effect on the critical speed. After studying their effects, the flutter speed was maximized by determining the best combination of the magnitude and location of the springs. Moreover, the effects of the variation of the center of gravity and mechanical damping were investigated. Finally, a plot of the variation of the real and imaginary parts of the eigenvalues with airspeed was obtained.

Table of Contents

List of Figures

List of Tables

Introduction

Aeroelasticity is the study of the interactions between inertia, elastic, and the aerodynamic forces occurring when an aeroelastic body undergoes a fluid flow. The occurrence of flutter can be defined as a self-excited vibration when the structure is under the interaction of inertial force, aerodynamic force, and elastic force. After the flutter has occurred, the aircraft structure demonstrates a limit cycle oscillation. This phenomenon can cause disastrous and fatal accidents or fatigue damage to the aircraft structures. Therefore, it is of great significance to study the aeroelastic characteristics of the structures for practical purposes. The analysis of the aeroelastic system helps in improving the stability of the aircraft structures.

This design project explores and studies the effects of aeroelasticity on the given wind tunnel model. The objective for this project is to use the quasi-steady incompressible aerodynamics, Newton equations, and lagrangian mechanics to derive the complete equations of motion to analyze the aeroelastic system illustrated in figure 2. The analysis of the aeroelastic model includes the computation of critical speeds (flutter and divergence) and studying the effects of the variation of spring coefficients, mechanical damping coefficient, C.G location (x_g), and the distances x_1 and x_2 on the computed critical speeds. Through this, we aim to gain a deeper understanding of the aeroelastic behavior under quasi-steady, incomprehensible, and uniform aerodynamic flow.

The given aeroelastic system consists of a combination of translational springs, a helical spring, mechanical damping, and a mass element. In the analysis, it is assumed that the incoming flow is uniform and subsonic. The problem statement states that the flow is also two dimensional and the system has a two-degree of freedom. The developed equations of motion are solved using Routh's stability criteria to determine the stability of the given aeroelastic system.

Computational Simulation and programming

This section will focus on the methods adopted to program the Matlab code to analyze the given aeroelastic system. Before programming the Matlab code it was essential to conceptualize the programming method for easier coding and debugging. The equations of motion were derived in part 1 with the help of Newton and Lagrange methods. These equations were then used to create a function in Matlab. The input variables for this function were the spring coefficients ($k_1, k_2, and\ k_{\theta 1}$), damping coefficient ($c_1$), their location with respect to the leading edge ($x_1, x_2, and\ x_c$), and the center of gravity location (x_g). Using the equation of motion and the characteristic equation, the function outputs the critical divergence and flutter speeds. This function called "criticalspeeds" solves the equations for the flutter and divergence speed. For parts 2 to 7, the function code was called to compute the required answers based on

various inputs. All the equations used in the function code are presented in the calculation section along with their descriptions.

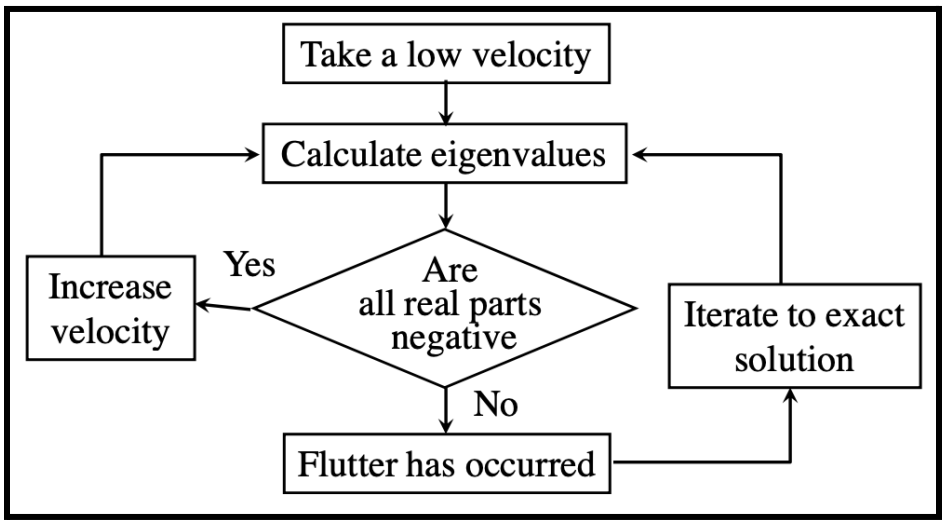

Figure 1: *Analysis Methodology.*

The figure above illustrates the block diagram of the methodology used to compute and analyze the flutter phenomenon. After calling the function described above, the characteristic equation is used to compute the eigenvalues for speeds 0 to 150 using a for loop. Initially , the program starts with a low velocity that is used to calculate the eigenvalues. The program then checks if all the real parts of the eigenvalues are negative. If the answer is yes then the speed is increased and the process is repeated. If the answer is negative then the flutter has occurred. To make this answer more accurate, the program iterates to the exact solution using smaller increments.

Calculations

Figure 2 below represents a two-dimensional, two-degree-of-freedom aeroelasticity model designed for wind tunnel testing. The model is a thin airfoil of unit span and chord "c" mounted in the wind tunnel via springs $k_1, k_2,\ and\ k_{\theta 1}$ and damping c_1. The airfoil has a mass "m" and a moment of inertia about the center of gravity. The aeroelastic analysis of the model is completed assuming that the incoming flow is uniform without any sudden gust or the presence of any shockwaves. The flow is inviscid and the boundary layer is not considered for the analysis. Furthermore, quasi-steady, incompressible aerodynamics is assumed for the aerodynamic forces calculations.

The essence of quasi-steady aerodynamics is that we account for bending and torsional motion by determining the equivalent induced velocity on the airfoil. We initially consider the airfoil undergoing vertical (h) and torsional (θ) motion. The h and θ are defined at some distance x_o from the leading edge. For the project, this distance (x_o) is the same as the mid-chord of the airfoil.

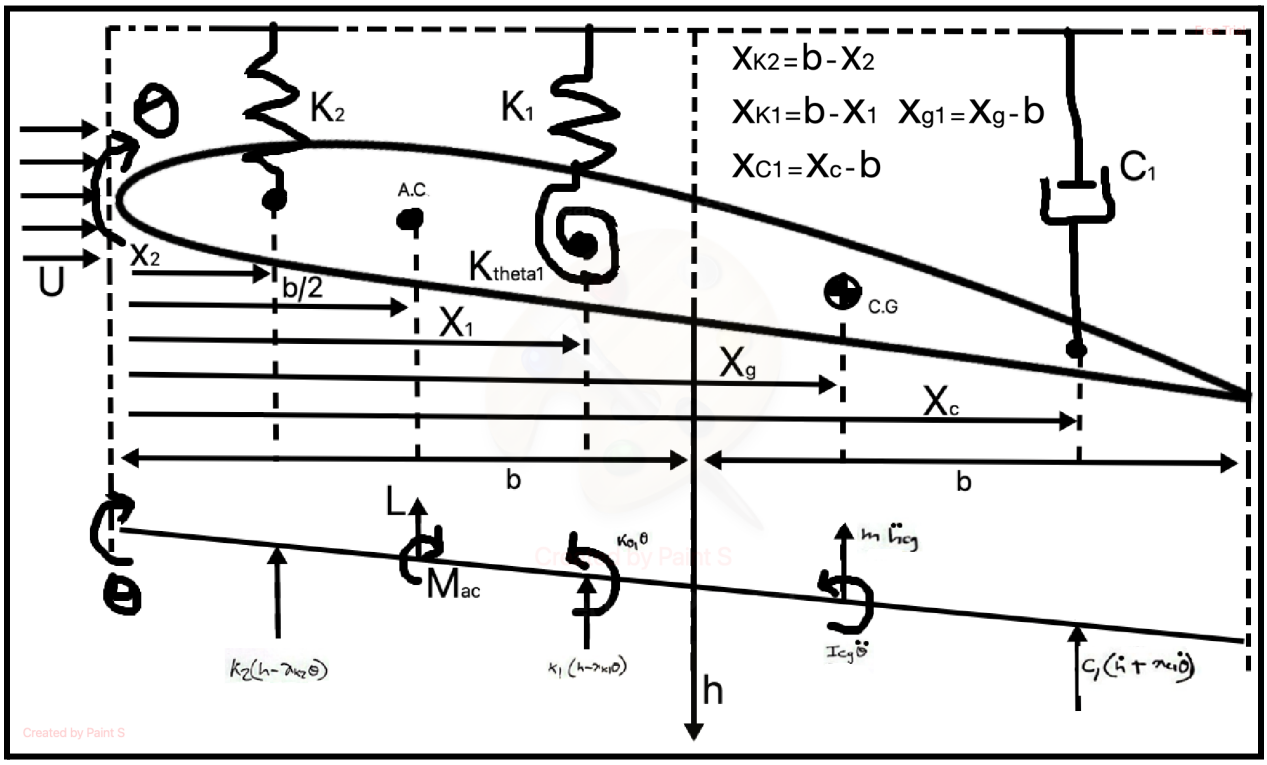

Figure 2: *Aeroelastic System.*

Newton Method

For the given aeroelastic system illustrated in figure 2, this section provides the calculations for the equations of motion using the newton method. This approach uses the classic summation of force and moments equal to zero to develop the equations of motion. The expressions with the springs represent the structural stiffness terms. The expressions with the damping represent the structural damping terms. The inertial terms represent the mass terms.

$$h_{c.g} = h + X_{g1}\theta \qquad \textit{Equation 1}$$

$$\dot{h}_{c.g} = \dot{h} + X_{g1}\dot{\theta} \qquad \textit{Equation 2}$$

$$\ddot{h}_{c.g} = \ddot{h} + X_{g1}\ddot{\theta} \qquad \textit{Equation 3}$$

$$\boldsymbol{F_h = 0;}$$

$$K_2\left(h - X_{k2}\theta\right) + K_1\left(h - X_{k1}\theta\right) + m\left(\ddot{h}_{c.g}\right) + C_1\left(\dot{h} - X_{c1}\dot{\theta}\right) = -L \qquad \textit{Equation 4}$$

$$m(\ddot{h}) + mX_{g1}(\ddot{\theta}) + C_1(\dot{h}) + (C_1 * X_{c1})(\dot{\theta}) + (K_1 + K_2)(h) + (-K_1 * X_{k1} - K_2 * X_{k2})(\theta) = -L \qquad \textit{Equation 5}$$

$$\boldsymbol{M_{M.C} = 0;}$$

$$K_2X_{k2}(h - X_{k2}\theta) + K_1X_{k1}(h - X_{k1}\theta) - K_{\theta 1}\theta - m\left(\ddot{h}_{c.g} * X_{g1}\right) - I_{c.g}\ddot{\theta} - C_1X_{c1}\left(\dot{h} - X_{c1}\dot{\theta}\right) + L\frac{b}{2} + M_{a.c} = 0 \qquad \textit{Equation 6}$$

$$(m * X_{g1})(\ddot{h}) + (m * X_{g1}^2 + I_{c.g})(\ddot{\theta}) + (C_1 * X_{c1})(\dot{h}) + (C_1 * X_{c1}^2)(\dot{\theta}) + (-K_1 * X_{k1} - K_2 * X_{k2})(h) + (K_2 * X_{k2}^2 + K_1 * X_{k1}^2 + K_{\theta 1})(\theta) = M_{a.c} + L\frac{b}{2} \qquad \textit{Equation 7}$$

Lagrangian Method

For the given aeroelastic system illustrated in figure 2, this section provides the calculations for the equations of motion using the Lagrangian method. This approach uses lagrangian equations, where T represents the kinetic energy, V represents the potential energy, q_i represents the independent generalized coordinates (in our case: h and θ), Q_i and represents the generalized forces (lift, moments, and damping).

$$\mathbf{T} = \frac{1}{2}\mathbf{m}\left(\dot{\mathbf{h}_{c.g}}\right)^2 + \frac{1}{2}\mathbf{I}_{c.g}\dot{\boldsymbol{\theta}}^2 = \frac{1}{2}\mathbf{m}(\dot{\mathbf{h}})^2 + \left(\mathbf{m} * \mathbf{X_{g1}}\right)\left(\dot{\mathbf{h}} * \dot{\boldsymbol{\theta}}\right) + \left[\frac{\mathbf{X_{g1}^2} * \mathbf{m}}{2} + \mathbf{I}_{c.g}\right](\dot{\boldsymbol{\theta}})^2 \qquad \textit{Equation 8}$$

$$\mathbf{V} = \frac{1}{2}\mathbf{K_2}(\mathbf{h} - \mathbf{X_{k2}}\boldsymbol{\theta})^2 + \frac{1}{2}\mathbf{K_1}(\mathbf{h} - \mathbf{X_{k1}}\boldsymbol{\theta})^2 + \frac{1}{2}\mathbf{K_{\theta 1}}\boldsymbol{\theta}^2 \qquad \textit{Equation 9}$$

$$\mathbf{W} = \mathbf{M_{a.c}} - \mathbf{L}\left(\mathbf{h} - \frac{\mathbf{b}}{2}\boldsymbol{\theta}\right) - \mathbf{C_1}(\dot{\mathbf{h}} + \mathbf{X_{c1}}\dot{\boldsymbol{\theta}})(\mathbf{h} + \mathbf{X_{c1}}\boldsymbol{\theta}) \qquad \textit{Equation 10}$$

$$\frac{\mathbf{d}}{\mathbf{dt}}\left(\frac{\partial \mathbf{T}}{\partial \dot{\mathbf{h}}}\right) + \frac{\partial \mathbf{V}}{\partial \mathbf{h}} - \frac{\partial \mathbf{T}}{\partial \mathbf{h}} = \mathbf{Q_h} = \frac{\partial \mathbf{W}}{\partial \mathbf{h}} \qquad \textit{Equation 11}$$

$$\boldsymbol{m}(\ddot{\boldsymbol{h}}) + \boldsymbol{mX_{g1}}(\ddot{\boldsymbol{\theta}}) + (\boldsymbol{K_1} + \boldsymbol{K_2})(\boldsymbol{h}) + (-\boldsymbol{K_1} * \boldsymbol{X_{k1}} - \boldsymbol{K_2} * \boldsymbol{X_{k2}})(\boldsymbol{\theta}) = -\boldsymbol{L} - \boldsymbol{C_1}(\dot{\boldsymbol{h}}) - (\boldsymbol{C_1} * \boldsymbol{X_{c1}})(\dot{\boldsymbol{\theta}}) \qquad \textit{Equation 12}$$

$$\frac{\mathbf{d}}{\mathbf{dt}}\left(\frac{\partial \mathbf{T}}{\partial \dot{\boldsymbol{\theta}}}\right) + \frac{\partial \mathbf{V}}{\partial \boldsymbol{\theta}} - \frac{\partial \mathbf{T}}{\partial \boldsymbol{\theta}} = \mathbf{Q_\theta} = \frac{\partial \mathbf{W}}{\partial \boldsymbol{\theta}} \qquad \textit{Equation 13}$$

$$(\boldsymbol{m} * \boldsymbol{X_{g1}})(\ddot{\boldsymbol{h}}) + (\boldsymbol{m} * \boldsymbol{X_{g1}^2} + \boldsymbol{I_{c.g}})(\ddot{\boldsymbol{\theta}}) + (-\boldsymbol{K_1} * \boldsymbol{X_{k1}} - \boldsymbol{K_2} * \boldsymbol{X_{k2}})(\boldsymbol{h}) + (\boldsymbol{K_2} * \boldsymbol{X_{k2}^2} + \boldsymbol{K_1} * \boldsymbol{X_{k1}^2} + \boldsymbol{K_{\theta 1}})(\boldsymbol{\theta}) = \boldsymbol{M_{a.c}} + \boldsymbol{L}\frac{\boldsymbol{b}}{\boldsymbol{2}} -$$

$$(\boldsymbol{C_1} * \boldsymbol{X_{c1}})(\dot{\boldsymbol{h}}) - (\boldsymbol{C_1} * \boldsymbol{X_{c1}^2})(\dot{\boldsymbol{\theta}}) \qquad \textit{Equation 14}$$

Part 1 - Equation of Motion

Now that we have completed the derivation of the L.H.S part of the equations of motion using the newton method and the Lagrangian method (equation 15), this section provides the calculations for the R.H.S i.e the aerodynamic damping and stiffness using the quasi-steady assumption. In quasi-steady aerodynamics we calculate this change in vorticity and the resulting lift and moment are represented by equations 16 and 17 respectively. The Quasi-steady lift and moment are functions of the time derivative of ‘θ’, the time derivative of ‘h’, and ‘θ’. The terms proportional to the displacement are stiffness terms and the expressions proportional to the vibrational velocity are damping terms.

$$\begin{bmatrix} m & m*X_{g1} \\ m*X_{g1} & m*X_{g1}^2 + I_{c.g} \end{bmatrix} \begin{Bmatrix} \ddot{h} \\ \ddot{\theta} \end{Bmatrix} + \begin{bmatrix} C_1 & C_1*X_{c1} \\ C_1*X_{c1} & C_1*X_{c1}^2 \end{bmatrix} \begin{Bmatrix} \dot{h} \\ \dot{\theta} \end{Bmatrix} +$$

$$\begin{bmatrix} K_1 + K_2 & -(K_1*X_{k1} + K_2*X_{k2}) \\ -(K_1*X_{k1} + K_2*X_{k2}) & K_2*X_{k2}^2 + K_1*X_{k1}^2 + K_{\theta 1} \end{bmatrix} \begin{Bmatrix} h \\ \theta \end{Bmatrix} = \begin{Bmatrix} -L \\ M_{a.c} + L\frac{b}{2} \end{Bmatrix} \quad \textit{Equation 15}$$

$$\mathbf{L = q * c * s\left\{2\pi\left[\theta + \frac{\dot{h}}{U} + \frac{\dot{\theta}}{U}\left(\frac{3}{4}c - X_o\right)\right]\right\} = q * c * s\left\{2\pi\left[\theta + \frac{\dot{h}}{U} + \frac{\dot{\theta}}{U}\left(\frac{b}{2}\right)\right]\right\}} \quad \textit{Equation 16}$$

$$M_{a.c} = q * c^2 * s\left[\frac{-2\pi * b}{8 * U}\dot{\theta}\right] \quad \textit{Equation 17}$$

$$\begin{bmatrix} -L \\ M_{a.c} + L\frac{b}{2} \end{bmatrix} = \begin{bmatrix} -q * c * s\left\{2\pi\left[\theta + \frac{\dot{h}}{U} + \frac{\dot{\theta}}{U}\left(\frac{b}{2}\right)\right]\right\} \\ q * c^2 * s\left[\frac{-2\pi * b}{8 * U}\dot{\theta}\right] + q * c * s\left\{2\pi\left[\theta + \frac{\dot{h}}{U} + \frac{\dot{\theta}}{U}\left(\frac{b}{2}\right)\right]\right\}\left(\frac{b}{2}\right) \end{bmatrix} \quad \textit{Equation 18}$$

$$\begin{bmatrix} -L \\ M_{a.c} + L\frac{b}{2} \end{bmatrix} = -2\pi qcs\left\{\frac{1}{U}\begin{bmatrix} 1 & \frac{b}{2} \\ -\frac{b}{2} & 0 \end{bmatrix}\begin{Bmatrix} \dot{h} \\ \dot{\theta} \end{Bmatrix} + \begin{bmatrix} 0 & 1 \\ 0 & -\frac{b}{2} \end{bmatrix}\begin{Bmatrix} h \\ \theta \end{Bmatrix}\right\} \quad \textit{Equation 19}$$

The mass matrix contains the mass elements and is represented by 'M'(eq. 20). The structural damping matrix consists of the damping terms. It is characterized by 'B_s'(eq. 21). The structural stiffness matrix contains the spring coefficient terms. It is characterized by 'E'(eq. 22). The aerodynamic damping matrix is represented by 'B_a'(eq. 23) and the aerodynamic stiffness is represented by 'K'(eq. 24). Equation 26 illustrates the complete equations of motion derived using the Newton and lagrangian method assuming the quasi-steady aerodynamics for the given aeroelastic system.

$$[M] = \begin{bmatrix} m & m * X_{g1} \\ m * X_{g1} & m * X_{g1}^2 + I_{c.g} \end{bmatrix}$$ *Equation 20*

$$[B_s] = \begin{bmatrix} C_1 & C_1 * X_{c1} \\ C_1 * X_{c1} & C_1 * X_{c1}^2 \end{bmatrix}$$ *Equation 21*

$$[E] = \begin{bmatrix} K_1 + K_2 & -(K_1 * X_{k1} + K_2 * X_{k2}) \\ -(K_1 * X_{k1} + K_2 * X_{k2}) & K_2 * X_{k2}^2 + K_1 * X_{k1}^2 + K_{\theta 1} \end{bmatrix}$$ *Equation 22*

$$[\mathrm{B_a}] = \begin{bmatrix} 1 & \frac{b}{2} \\ -\frac{b}{2} & 0 \end{bmatrix}$$ *Equation 23*

$$[\mathrm{K}] = \begin{bmatrix} 0 & 1 \\ 0 & -\frac{b}{2} \end{bmatrix}$$ *Equation 24*

$$\mathrm{f_1(U)} = \frac{2\pi qcs}{\mathrm{U}};\ \mathrm{f_2(U)} = 2\pi qcs$$ *Equation 25*

$$[\mathrm{M}]\begin{Bmatrix} \ddot{h} \\ \ddot{\theta} \end{Bmatrix} + ([\mathrm{B_s}] + \mathrm{f_1(U)}[\mathrm{B_a}])\begin{Bmatrix} \dot{h} \\ \dot{\theta} \end{Bmatrix} + ([\mathrm{E}] + \mathrm{f_2(U)}[\mathrm{K}])\begin{Bmatrix} h \\ \theta \end{Bmatrix} = \begin{Bmatrix} 0 \\ 0 \end{Bmatrix}$$ *Equation 26*

The next step is to solve the formulated equations of motions via Routh's stability criteria to determine the critical flutter speed and the system stability. The combined bending/torsional equations can be solved by assuming solutions to h and θ of the form,

$$h = h_o e^{\lambda t} \; and \; \theta = \theta_o e^{\lambda t}$$

$h_o \; and \; \theta_o$ represent the amplitude of vibration and λ the system eigenvalue. In general $h_o, \theta_o \; and \; \lambda$ are complex numbers. h_o/θ_o is the system eigenvector and gives the relative magnitude of $h \; and \; \theta$ motion and the phase difference between them. Assuming $\lambda = \lambda_R + i\lambda_i$ represents the solution for the eigenvalues, the imagery part λ_i shows the oscillatory part of the motion and the real part λ_R shows if the amplitude is decaying or growing. The system's stability is given by the eigenvalues and how it varies with the velocity.

$$\{[\boldsymbol{M}]\boldsymbol{\lambda}^2 + ([\boldsymbol{B_s}] + \boldsymbol{f_1(U)}[\boldsymbol{B_a}])\boldsymbol{\lambda} + ([\boldsymbol{E}] + \boldsymbol{f_2(U)}[\boldsymbol{K}])\}\begin{Bmatrix}\boldsymbol{h_o}\\ \boldsymbol{\theta_o}\end{Bmatrix}\boldsymbol{e^{\lambda t}} = \begin{Bmatrix}\mathbf{0}\\ \mathbf{0}\end{Bmatrix} \quad \textit{Equation 27}$$

$$\boldsymbol{P_4\lambda^4 + P_3\lambda^3 + P_2\lambda^2 + P_1\lambda + P_o = 0} \quad \textit{Equation 28}$$

$$\mathbf{P_4 = 0.25} \quad \textit{Equation 29}$$

$$\mathbf{P_3 = \frac{97}{320} + \frac{49\pi U}{1024}} \quad \textit{Equation 30}$$

$$\mathbf{P_2 = \frac{29975}{8} - \frac{49\pi U^2}{320} + \frac{2401(\pi U)^2}{409600} + \frac{441\pi U}{32000}} \quad \textit{Equation 31}$$

$$\mathbf{P_1 = 1550 + \frac{14651\pi U}{32} - \frac{539\pi U^2}{3200}} \quad \textit{Equation 32}$$

$$\mathbf{P_o = 8810000 - \frac{3185\pi U^2}{16}} \quad \textit{Equation 33}$$

The divergence critical speed can be calculated by equating $P_o = 0$. The flutter critical can be calculated with the following equation:

$$\mathbf{T_3 = P_1P_2P_3 - P_1^2P_4 - P_oP_3^2 = 0} \quad \textit{Equation 34}$$

The table below tabulates the given data for the aeroelastic wind tunnel model. This data is used for the calculation of flutter and divergence speeds. Furthermore, the stability of the system is computed for three different speeds to illustrate the behavior of the aeroelastic model.

Table 1: *Given Data*

Parameter	Magnitude
Chord (c)	0.5 m
(U_{max})	$150\ \frac{m}{s}$
(k_1)	$7\ \frac{KN}{m}$
(k_2)	$8\ \frac{KN}{m}$
$(k_{\theta 1})$	$550\ \frac{N.m}{rad}$
(c_1)	$1\ \frac{N.s}{m}$

(x_1)	0.2 m
(x_2)	0.1 m
(x_c)	0.4 m
(x_g)	0.175 m
m	5 Kg
$(I_{C.G})$	$0.05\ Kg.m^2$

Part 2 - Routh's Stability Criteria

The Routh-Hurwitz stability criterion is a mathematical test performed to determine the stability of the developed equations of motion. The examples below use three different speeds: 15, 25, and 37.1 m/s, to demonstrate the behavior of the aeroelastic system and analyze the stability of the system at these speeds. The characteristic equation developed in equation 28 is used with the above-mentioned speeds to solve Routh's table. The coefficients of the characteristic equation must all be positive and greater than zero. The stability of the system is ensured provided that there is no change in the sign in the first column of Routh's table. The dynamic stability boundary is given by equation 34.

Table 2: *Routh's Stability Criteria for U = 15 m/s*

λ^4	P_4	P_2	P_0
λ^3	P_3	P_1	
λ^2	1403.83	8669291.01	
λ^1	7209.5	0	
λ^0	8669291.01		

For the speed of 15 m/s, there is no change of sign in the first column. Therefore, the aeroelastic model is stable at U = 15 m/s.

Table 3: *Routh's Stability Criteria for U = 25 m/s*

λ^4	P_4	P_2	P_0
λ^3	P_3	P_1	
λ^2	1194.15	8419141.7	
λ^1	8554	0	
λ^0	8419141.7		

For the speed of 25 m/s, there is no change of sign in the first column. Therefore, the aeroelastic model is stable at U = 25 m/s. The dynamic stability of the system is given by equation 34. Therefore solving this equation gives the flutter speed of 37.087 m/s. The static stability of the aeroelastic model is given by equation 33. The divergence speed was calculated as 118.7 m/s.

Table 4: *Routh's Stability Criteria for U = 37.1 m/s*

λ^4	P_4	P_2	P_0
λ^3	P_3	P_1	
λ^2	862.2	7949229.95	
λ^1	-27.1	0	
λ^0	7949229.95		

For the speed of 37.1 m/s, there is a change of sign in the first column. Therefore, the aeroelastic model is unstable at U = 37.1 m/s. This indicates that the model undergoes flutter before this speed and the system becomes unstable. Routh's stability criteria can be performed for speeds 0 to 150 to determine the system stability for this range. The positive stability indicates that the system will have a negative real part for all the eigenvalue solutions of the characteristic equation. The negative stability indicates that the system will have at least one positive real for the eigenvalue solutions of the characteristic equation.

Results

Part 2

This section presents the results from the MATLAB code developed to analyze the given aeroelastic system. From the developed equations of motion and the characteristic equation, the eigenvalues were computed for speeds 0 to 150 m/s. The dynamic stability boundary was calculated with equation 34 and the static stability boundary was calculated with equation 33. The critical Flutter speed for the given aeroelastic wind tunnel model is calculated to be 37.087 m/s. The critical divergence speed was calculated to be 118.7 m/s.

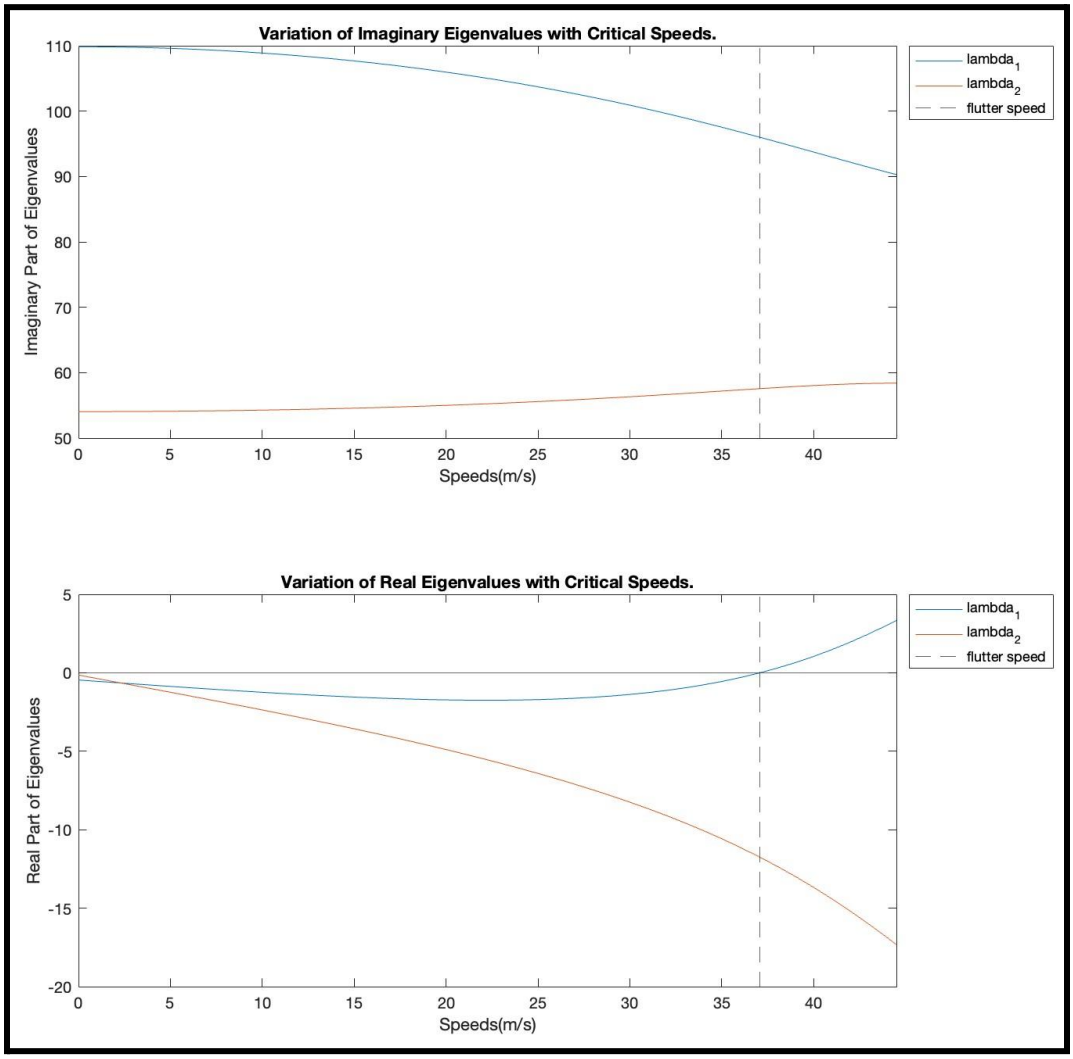

Figure 3: *Variation of Real and Imaginary Parts of Eigenvalues with Critical Flutter Speed.*

The figure above illustrates the variation of the real and imaginary parts of the eigenvalues calculated for part b with the critical flutter speed. As seen in the figure, in the instance of flutter, the real part of the eigenvalue (λ_1) is exactly zero. Beyond this speed, the eigenvalue (λ_1) has a positive real part, and thus, the system becomes unstable.

Part 3

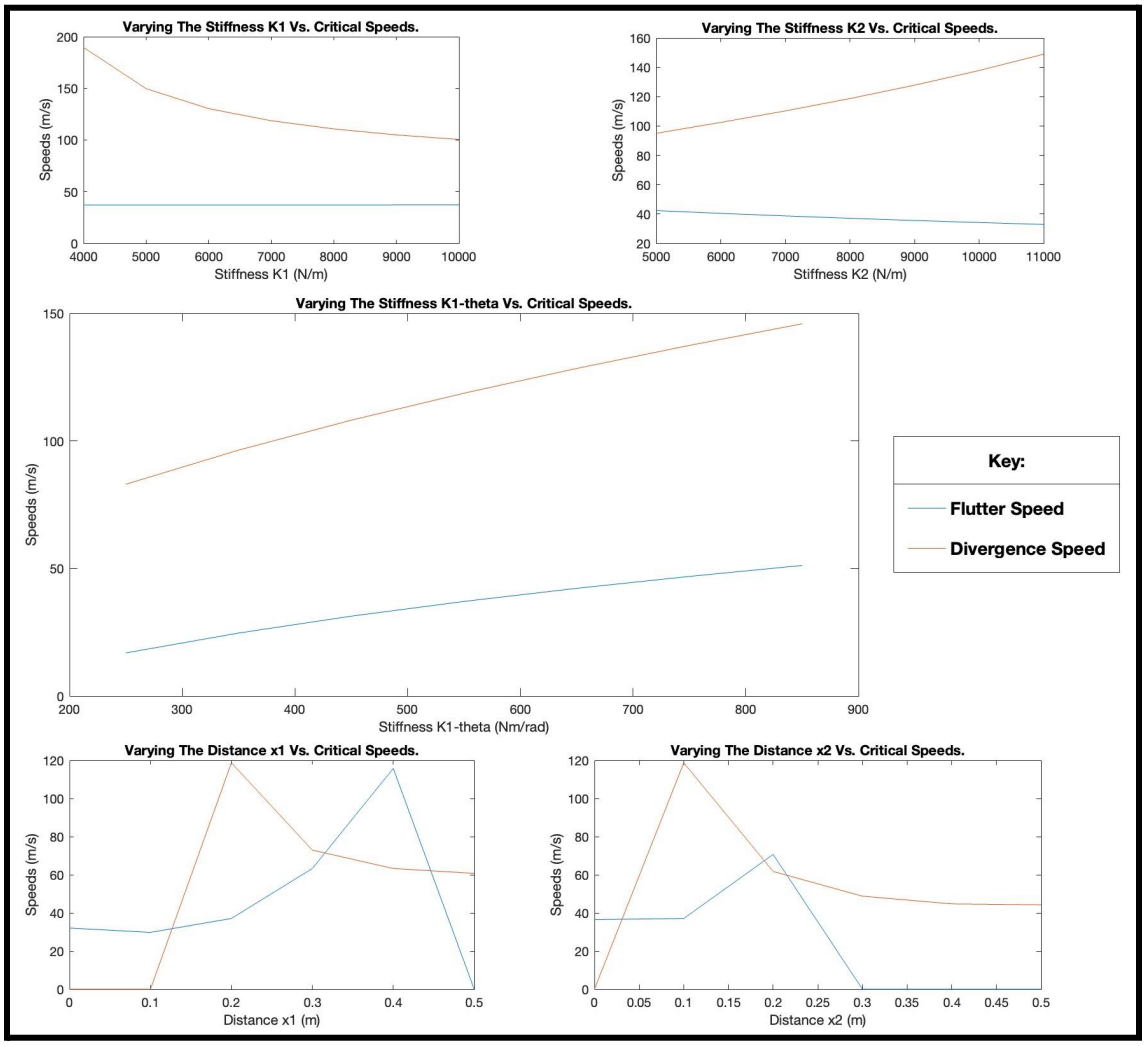

Figure 4: *Variation of Critical Speeds with Various Magnitudes of Spring Constants and Distances.*

The figure above illustrates the variation of the critical speeds (flutter and divergence) with various magnitudes of spring constants and their respective distances from the leading edge. This analysis is important to determine the best design combination of $k_1, k_2, k_{\theta 1}, \ and \ x_1$ for the maximum critical speeds. The critical speeds are calculated and then plotted for 7 different stiffness coefficients for the first three plots. The effect of the critical speeds is computed by varying the distances of the springs along the chord of the airfoil.

The first plot in the above figure shows the effect of the variation of spring stiffness K_1 on the critical flutter and divergence speeds. The critical flutter speed remains approximately constant with the biggest deflection of 0.3% when $K_1 = 10000\, N/m$ compared to the above-calculated flutter value. The critical divergence speed decreases as the stiffness increases, which is evident in the plot. The second plot illustrates the effect of the variation of spring stiffness K_2 on the critical divergence and flutter speeds. As the stiffness is decreased, the critical flutter speed also decreases. Whereas, as the stiffness is decreased, the critical divergence speed increases having an inverse relationship. The third plot illustrates the effect of the variation of spring stiffness $K_{\theta 1}$ on the critical divergence and flutter speeds. As the stiffness coefficient of the helical spring is increased, the critical flutter and divergence speeds also increase.

The fourth plot illustrates the effect of the variation of x_1 (the position of the translational spring 1 and helical spring 1) on the critical divergence and flutter speeds. The distance x_1 is moved along the chord of the airfoil to analyze this effect. As the distance x_1 increases, the flutter speed also increases until it reaches a maximum of 115.7 m/s at $x_1 = 0.4m$. After which, there is no flutter which is indicated by a '0' in the graph. There could be flutter at higher speeds than the prescribed maximum velocity but it is out of the scope of this analysis. Similarly, there is no divergence problem from $x_1 = 0\ to\ 0.1$. This is because the elastic axis location becomes negative for the static analysis. After this point, the critical divergence speed decreases as the position of x_1 moves towards a trailing edge.

The fifth plot illustrates the effect of the variation of x_2 (the position of the translational spring 2) on the critical divergence and flutter speeds. The distance x_2 is moved along the chord of the airfoil to analyze this effect. The critical flutter speed increases as the distance x_2 increases up to $x_2 = 0.2\, m$. After this point, there is no flutter which is indicated by a '0' in the graph. On the other hand, if the translational spring 2 is placed at the leading edge ($x_2 = 0$) there is no divergence since the elastic axis becomes negative for the static analysis. After this point, the divergence decreases as the location of x_2 moves towards the trailing edge.

Part 4

In this section, the best combination of $k_1, k_2, k_{\theta 1}, and\ x_1$ is designed for the maximum critical speed. When the flutter speed is maximized, the divergence speed tends to decrease. The opposite is true as well. Therefore, three different iterations are performed. In the first iteration, only the flutter speed is maximized by obtaining a suitable combination of the design parameters. In the second iteration, only the divergence speed is maximized. In the third iteration, a combination of the design parameters is obtained such that both divergence and flutter speed is maximized.

Iteration 1: Maximizing Flutter Speed

To design the best combination of $k_1, k_2, k_{\theta 1}, and\ x_1$ for the maximum critical flutter speed, it is important to analyze the effect of every single element on the critical flutter speed. This effect is analyzed using figure 4. However, the sum of spring constants must be less than 16000 N/m, and each spring must be greater than 1000 N/m. Along with this, $k_{\theta 1}$ should be less than 7000 Nm/rad and x_1 greater than 0.2m. The critical flutter speed can be maximized by increasing $k_1\ and\ k_{\theta 1}$, decreasing k_2, and moving the location of $x_1\ close\ to\ 0.25\ m$. Therefore, considering the constraints on $k_1, k_2, k_{\theta 1}, and\ x_1$ the computed values are as follows.

Table 5: *Computed Values for $k_1, k_2, k_{\theta 1}, and\ x_1$ to maximize Critical Flutter Speed*

Parameter	**Magnitude**
k_1	14,000 N/m
k_2	2,000 N/m
$k_{\theta 1}$	699 Nm/rad
x_1	0.251 m

The critical flutter speed for the above-selected parameters is computed to be 149.65 m/s. The critical divergence speed for the above-selected parameters is computed to be 59.8715 m/s. The critical flutter speed could be maximized further; however, it will exceed the maximum speed allowed for the given model. Therefore, this represents the maximum critical flutter speed for the model within the flight envelope.

Iteration 2: Maximizing Divergence Speed

In the second iteration, the critical divergence speed is maximized. From figure 4, it can be observed that the divergence speed decreases as the k_1 increases, and the divergence speed increases as the k_2 value is increased. Moreover, the divergence speed is at its max close to an x_1 value of 0.2. Therefore, by finding the best combinations of these parameters, the maximum divergence speed can be determined. The following table lists the optimal design parameters for the maximum critical divergence speed.

Table 6: *Computed Values for $k_1, k_2, k_{\theta 1}$, and x_1 to maximize Critical Divergence Speed*

Parameter	**Magnitude**
k_1	6,000 N/m
k_2	10,000 N/m
$k_{\theta 1}$	699 Nm/rad
x_1	0.213 m

The critical divergence speed obtained utilizing the design parameters above is 149.4638 m/s. The divergence speed could be maximized further; however, it will exceed the maximum speed allowed for the given model. The flutter speed obtained with the above design parameters is approximately 43.224 m/s. In general, the trend can be observed that when either the divergence or flutter speed is maximized, the other speed decreases simultaneously.

Iteration 3: Maximizing both Flutter and Divergence Speed

In the final iteration, the optimum combination of the design parameters are obtained by maximizing both the flutter and divergence speed. When both are maximized simultaneously at the optimum point, the lower speed will be the critical speed of the wing model.

Table 7: *Computed Values for $k_1, k_2, k_{\theta 1}, and\ x_1$ to maximize Critical Flutter and Divergence Speed*

Parameter	**Magnitude**
k_1	8,000 N/m
k_2	8,000 N/m
$k_{\theta 1}$	699 Nm/rad
x_1	0.31 m

Using the above combination of design parameters, the divergence and flutter speed are computed to be 75.4102 m/s and 77.0161 m/s, respectively. Hence, the divergence speed represents the critical speed since it is lower than the flutter speed.

Part 5

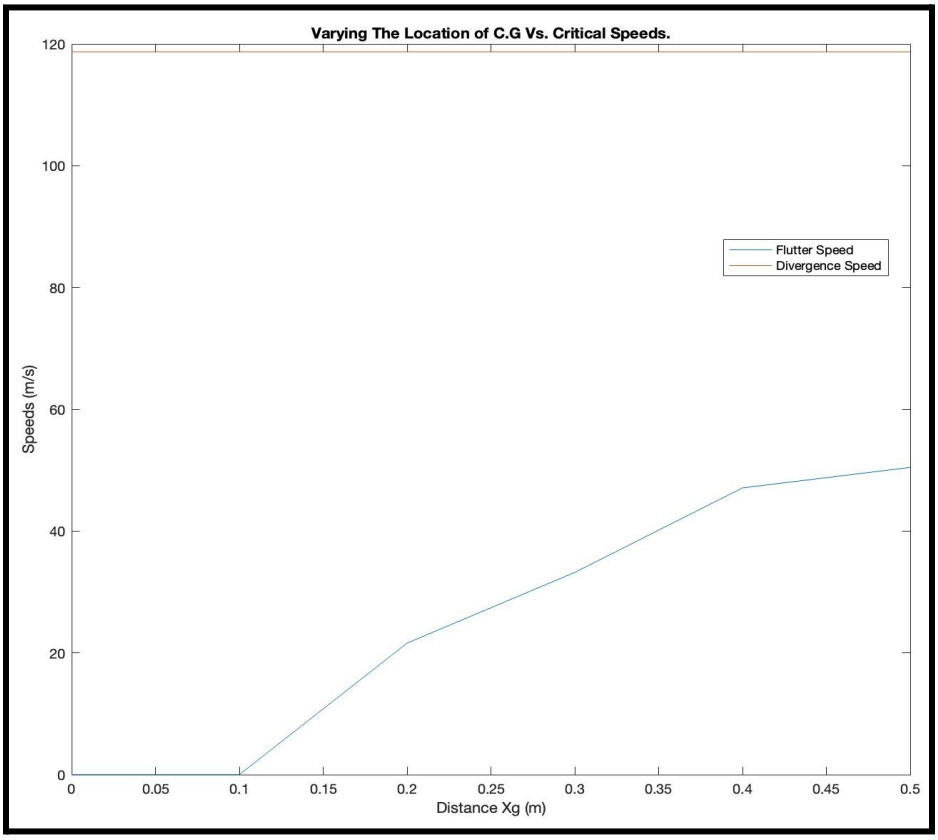

Figure 5: *Variation of Critical Speeds with C.G location.*

The figure above illustrates the effect of the variation of the C.G. location along the chord of the airfoil on the critical speeds. As seen in the figure, the change in the C.G. location has no effect on the critical divergence speed. This is because the static aeroelastic stability analysis does not account for the inertial terms. On the other hand, there is no flutter problem from $x_g = 0\ to\ 0.1m$. This is usually true when the elastic axis is before the center of gravity. Beyond this point, the critical flutter speed increases as the x_g location approaches the trailing edge. To maximize the critical flutter speed, the proposed location for the center of gravity is at the trailing edge of the airfoil. At the trailing edge ($x_g = 0.5m$) the critical flutter speed is calculated to be 50.45 m/s.

Part 6

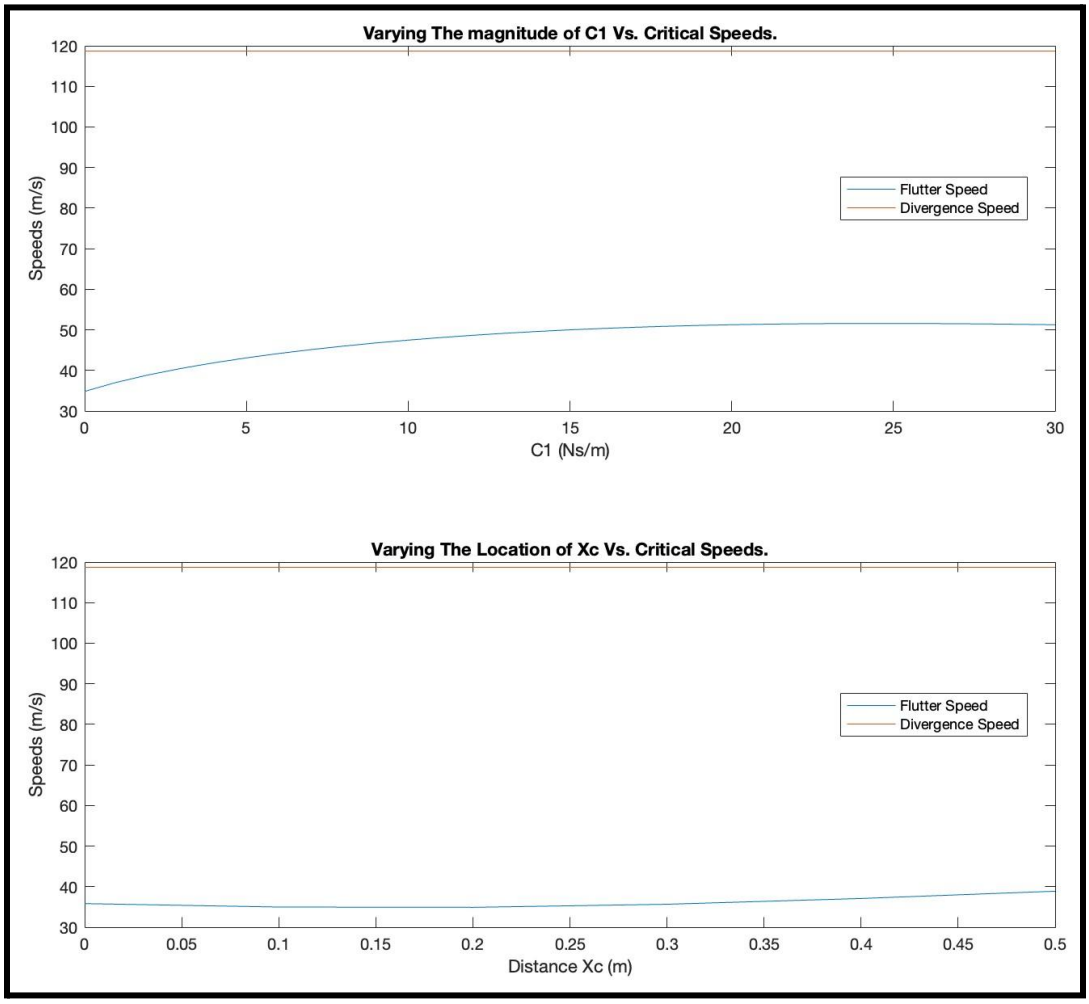

Figure 6: *Variation of Critical Speeds with Damping Coefficient and Distances.*

The figure above illustrates the effect of the variation of the coefficient of mechanical damping and its location (x_c) on the critical divergence and flutter speeds. The critical divergence speed does not change with the change in the mechanical damping coefficient and its location (x_c). This is because the static aeroelastic stability analysis does not account for the damping terms. The critical flutter speed increases with the increase in the mechanical damping coefficient. This is because as the structural damping term increases, the system's damping stabilizes faster which decreases the chance of flutter occurring at lower airspeeds. The maximum critical flutter speed occurs at $C_1 = 30\ Ns/m$. The critical flutter speed decreases as the location of the mechanical damping increases until $x_c = 0.2m$. After this point, the critical flutter speed increases as the location of the mechanical damping approaches the trailing edge location.

Part 7

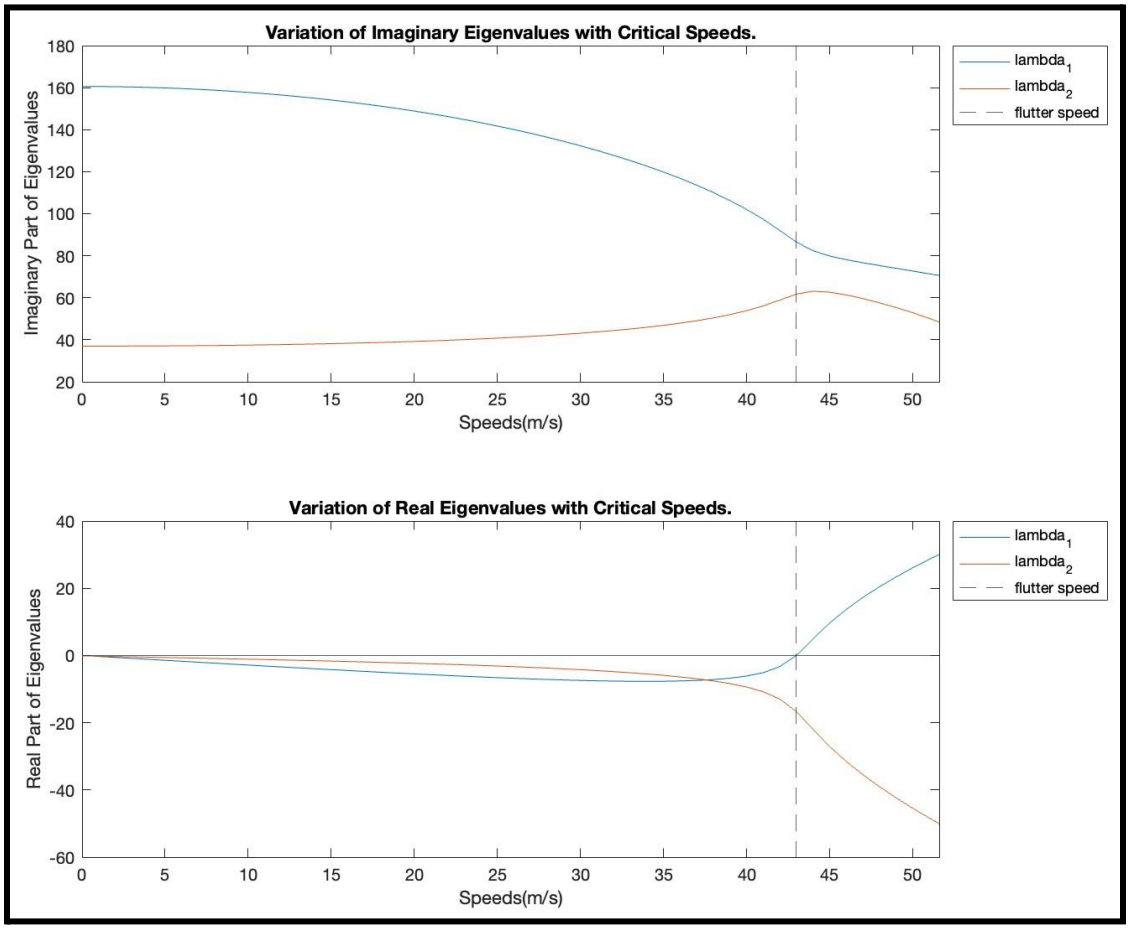

Figure 7: *Variation of Real and Imaginary Parts of Eigenvalues with Critical Flutter Speed for part 7.*

The figure above illustrates the variation of the real and imaginary parts of the eigenvalues versus airspeed up to 1.2 times the critical speeds. The above graph was computed with values similar to that in part 2 expect $x_g = 0.35m$. As seen in the figure, in the instance of flutter, the real part of the eigenvalue (λ_1) is exactly zero. Beyond this speed, the eigenvalue (λ_1) has a positive real part and thus, the system becomes unstable. Before the instance of flutter, the real part of the eigenvalues is negative, representing that the system is stable. The critical speeds were computed using similar methods as for part 2. The critical flutter speed was computed to be 43 m/s. Whereas, the divergence speed was calculated to be 118.7 m/s.

Analysis

The project focuses on the dynamic aeroelastic analysis of the given two-dimensional airfoil model. The analysis includes the computation of critical flutter and divergence speeds. When the aircraft airspeeds are increased to the computed critical value, the amplitude of the structural vibration remains constant. At this point and beyond, the structure undergoes a limit cycle oscillation. This is the physical indication of flutter. The flutter can cause catastrophic and fatal accidents. For parts 2 and 7, it was observed that the flutter speeds were computed to be less than the divergence speeds. This means that the flutter occurs before the divergence phenomenon. The occurrence of flutter describes the state of wing deformation in the form of its oscillation. The occurrence of divergence after the flutter indicates that the aerodynamic forces are more than the restoring forces from the structural stiffness.

Through the aeroelastic analysis, it was observed that the speed at which this flutter occurs may be increased by increasing the torsional stiffness, increasing the structural damping, moving the elastic axis back (just aft of the a.c.), decreasing the moment of inertia and moving the C.G. axis back. However, the impact of implementing such solutions might impact the stability and weight of the aircraft itself. Furthermore, it was observed that the coupling between the bending and torsional modes has a strong effect on the flutter speed. This can be characterized by static unbalance of the airfoil or the distance between the center of gravity and the elastic axis.

The divergence problem can be solved by making the aircraft wing structure as stiff as possible. However, this would increase the weight of the wing structure. It was also observed that the critical flutter speeds can be increased by maximizing the initial frequency difference between the bending and torsion modes. The initial frequency difference can be maximized by maximizing the difference between the complex parts of the eigenvalues.

It was observed that the critical flutter speed remains marginally constant as the stiffness of spring 1 is increased. Whereas, the critical flutter speed decreases as the stiffness of spring 2 is increased. The critical flutter speed increases with the increase in the stiffness of the helical spring. This is because the two translational springs and the helical spring contribute to the structural stiffness matrix in the equations of motion. The solution for the characteristic equation results in four eigenvalues as a function of airspeed. The real part represents the stability of the system and the imaginary part represents the frequency of oscillation of the motion. As the airspeed is increased, the two modes, which are initially distinct become almost equal. This is seen in figure 3 in part 2 and figure 7 in part 7.

Conclusion

Overall, the project was successful in demonstrating the response of the aeroelastic model under quasi-steady incompressible aerodynamic conditions. It was also proven that Newton's Equations and Lagrange Mechanics output the same answer of the equation of motion. The critical flutter speed at the given design parameters was calculated to be 37.1 m/s. By varying the stiffness and location of the spring, the variation of the critical speeds with respect to each design parameter was plotted. In addition, the critical divergence speed and critical flutter speed were both maximized by determining the best combination of the design parameters. In addition, it was also determined how the variation of the center of gravity and mechanical damping affected the critical speeds of the system. Finally, the variation of the real and imaginary parts of the eigenvalues was plotted versus airspeed.